ELSEVIER

Aerospace Science and Technology 6 (2002) 131–145

Aerospace Science and Technology

www.elsevier.com/locate/aescte

A new micromechanics based CDM model and its application to CMC's

J.-L. Chaboche, J.-F. Maire

ONERA, DMSE, 29, Av. de la Division Leclerc BP72, F-92322 Châtillon Cedex, France

Received 6 April 2001; received in revised form 3 January 2002; accepted 8 January 2002

Abstract

A CDM theory is further developed in order to better model the non linear and dissipative behavior of Ceramic Matrix Composites. A new damage deactivation rule is developed, directly based on mechanics of microcrack behavior, considering both closure effects and the corresponding elastic energy storage. The complete model uses two sets of damage state variables, the scalar ones correspond to microcracks oriented by reinforcements and a second order tensor that evolves with the maximum principal strain directions. The model is applied to uniaxial and multiaxial monotonic and cyclic tests on a SiC/SiC composite. In addition, the new version of the damage deactivation rule allows a progressive effect and a better description of the residual strain.

Keywords: Mechanical behavior; Damage mechanics; Constitutive modeling; Composite materials; Ceramic matrix composites

1. Introduction

The Continuum Damage Mechanics (CDM), as a purely macroscopic tool, do not try to describe all the local, micromechanical and physical features but summarizes and approximates them through global constitutive and damage equations. Since the pioneering work of Kachanov [21] many progresses have been done in the development of a consistent continuum framework and its application to numerous materials.

One of the difficult subjects in CDM modeling is the simultaneous description of damage induced anisotropy and the damage deactivation effects that appear under unloadings and compressive-like loading conditions. (1) 各向异性损伤研究历史 Concerning damage induced anisotropy, works done during the eighties were introducing damage vectors [23], second order tensors [12, 32], or fourth order tensors [5,20]. Let us recall that the idea of a second order tensor was also proposed by Kachanov and Vakulenko [36], based on a micro-macro analysis for a microcracked elastic materials. The last category, a fourth order damage tensor, is probably necessary in the case of an initially isotropic material, when the microcracks, oriented by the applied stress (or strain) direction, induce a clear anisotropy of the subsequent material behavior. However, in the present paper, where the material is initially anisotropic,

本文假设材料初始各向异性

and where a significant amount of microcracks is oriented by the composite reinforcements, we decide to limit the damage description to a set of scalar variables and one second rank damage tensor. The reason for such a limitation will appear in the subsequent model developments. One of them is to use a fourth rank damage effect tensor that depends linearly on the second order damage tensor.

采用一组标量
二阶张量描述

其中一组模型
采用一个四阶
张量描述损伤

Concerning composite materials, damage models have been developed at several scales during the last decade, using various approaches. One of the most powerful for structural applications is developed at the mesoscale, considering for instance each ply of a composite laminate as a continuum. We can mention the works done by Talreja [35], and the Ladeveze approach [24,26]. There are also many attempts to model composite materials and structures at various microscales (fiber, matrix, bundles, plies, interfaces ...) using both fracture mechanics and interface damage mechanics concepts, but these aspects will not be developed in the present paper.

复合材料CDM模

The presentation focuses here on the case of CMC's, especially SiC/SiC composites, where the available ductility is essentially due to matrix microcracking and debonding and friction at the fiber/matrix interfaces. Moreover, in such composites the damage deactivation effects are extremely pronounced, which need to focus a special attention to the application and validity range of the corresponding deactivation rules. Section 2 summarizes the general lines of the followed CDM approach and gives the constitutive and dam-

第二节的CDM模型只适用于非卸载情况。
第三节将第二节的模型与试验数据对比。
第四节研究了卸载的情况。
第五和第六节对新模型进行了讨论。

E-mail address: chaboche@onera.fr (J.-L. Chaboche).

1270-9638/02/$ – see front matter
PII: S1270-9638(02)01154-9

age model for CMC's applications, limiting the presentation to the particular case where damage is active. The general applicability of the model is checked Section 3 by comparisons with several simple or complex experiments made on a SiC/SiC composite, including multiaxial tests realized on tubular specimens under tension/torsion or tension/internal pressure.

Section 4 discusses the difficult problems associated with the damage deactivation conditions. We explain some deficiencies of a condition used previously at Onera [6,7,9,30] that was able to preserve the continuity of the stress-strain response for general complex multiaxial loading conditions. A new formulation is then proposed, based on micromechanics arguments. In Section 5 some applications are given for SiC/SiC composites, that demonstrate the improvements and additional modeling capabilities associated with the new deactivation methodology. We also propose a generalized formulation that introduces a progressive deactivation. The present modeling capabilities and future developments concerning the implementation of damage induced friction effects are then discussed in Section 6.

2. General constitutive and damage framework

本节只讨论不卸载的情况，卸载的情况在第四节讨论。

In this section, we summarize the developed model for its application to Ceramic Matrix Composites. The formulation is shown considering only conditions for active damage, in order to extract the essential modeling features and to recall the general thermodynamic framework.

The composite material is modeled at the mesoscale level, as a continuum. In case of laminated structures for example, each ply is treated as a different material, with its own constitutive and damage equations, the laminate model being then obtained through the structural analysis. To describe delamination between plies, as in many other work, we assume damaging interfacial layers. However, the basic configuration considered here applies for a composite representative volume element, treated as homogeneous at the mesoscale. For CMC's it will be the superposition of several woven plies.

前面都是废话，现在正式开始CDM理论框架。

The model is built up in the general framework of continuum thermodynamics with internal variables. In the present context, the main independent internal state variables are the damage variables, either scalars, second order or fourth order tensors. We presently limit ourselves to scalars δ_α, $\alpha = 1, 2, \ldots, N$, and one second order tensor $\boldsymbol{d}$. The higher order anisotropies are being given by fourth order material dependent tensors, related to the composite microstructure. Variables δ_α correspond to families of microcracks that develop parallel to the reinforcements, as the woven bundles. On the contrary, the second order damage $\boldsymbol{d}$ involves three orthogonal families of microcracks, for which directions are not necessarily given by the reinforcements. Such a tensorial variable represents at the macroscopic level those microcracks which evolutions are driven by the maximum principal strain (or stress).

The thermodynamics based CDM approach then considers two potentials:

- the *state potential* that contains all information relative to the elastic behavior, including the damage effect and damage deactivation effects. It is formulated in terms of the elastic strain as the observable variable, but the dual stress formulation also exists, equivalent for low damage values. An inelastic strain ε_{in}, containing several terms, will play role when incorporating deactivation and friction effects and also residual strains associated with the manufacturing process and the development of damage. Table 1 indicates the specific choices made for Ceramic Matrix Composites, in the situation where damage effects are all active (only open microcracks). Damaged Hooke's law of the material is obtained directly by derivation, as well as the thermodynamic forces associated with damage variables (called respectively y_α and $\boldsymbol{y}$). The present formulation of the state law has been guided by micromechanics considerations. The potential expression in Table 1, at least in the case where ε_{in} is neglected, can be considered as the dual expression from the ones that are available for solid containing many microcracks (see for example Kachanov [22]).
- the *dissipative potential*, written in the space of thermodynamic forces, that allows to respect directly the second law of thermodynamics by using the corresponding

Table 1
The state potential and the thermodynamic forces for the completely active damage

$$\psi(\varepsilon) = \frac{1}{2}\left(\varepsilon - \varepsilon^{\text{th}} - \varepsilon^{\text{r}}\right) : \widetilde{\boldsymbol{C}} : \left(\varepsilon - \varepsilon^{\text{th}} - \varepsilon^{\text{r}}\right) \tag{1}$$

$$\widetilde{\boldsymbol{C}} = \boldsymbol{C} - \sum_{\alpha=1}^{m} \delta_\alpha \boldsymbol{K}_\alpha - \left[\boldsymbol{D}(\boldsymbol{d}) : \boldsymbol{K}\right]_s \qquad \boldsymbol{D}(\boldsymbol{d}) = \gamma(\mathbf{1} \otimes \boldsymbol{d})_s + \frac{\gamma - 1}{2}(\mathbf{1} \underline{\otimes} \boldsymbol{d} + \mathbf{1} \overline{\otimes} \boldsymbol{d})_s \tag{2}$$

$$\sigma = \widetilde{\boldsymbol{C}} : \left(\varepsilon - \varepsilon^{\text{th}} - \varepsilon^{\text{r}}\right) \tag{3}$$

$$y_\alpha = -\frac{\partial \psi}{\partial \delta_\alpha} = \frac{1}{2}\left(\varepsilon - \varepsilon^{\text{th}} - \varepsilon^{\text{r}}\right) : \boldsymbol{K}_\alpha : \left(\varepsilon - \varepsilon^{\text{th}} - \varepsilon^{\text{r}}\right) \tag{4}$$

$$\boldsymbol{y} = -\frac{\partial \psi}{\partial \boldsymbol{d}} = \frac{\gamma}{4}\left(\bar{\varepsilon}\,\mathrm{Tr}(\bar{\sigma}) + \bar{\sigma}\,\mathrm{Tr}(\bar{\varepsilon})\right) + \frac{1-\gamma}{2}(\bar{\sigma}.\bar{\varepsilon})_s \quad \text{with } \bar{\varepsilon} = \varepsilon - \varepsilon^{\text{th}} - \varepsilon^{\text{r}},\ \bar{\sigma} = \boldsymbol{K} : \bar{\varepsilon} \tag{5}$$

normality rules. In the present context we do not follow a completely associated rule, considering the possible dependency of the dissipative potential upon other state variables (considered as parameters). In practice, for rate independent conditions, this potential is taken as the indicatrice function of the "non-damage" domain, the one inside which thermodynamic force evolutions do not produce any damage growth (like the elastic domain in standard plasticity). Therefore, thermodynamic arguments and associated dissipated energies, are used essentially in order to limit the range of possible choices for the damage rates. Moreover, the chosen expressions do not respect micromechanics quantitatively, as shown for instance by Kachanov [22]. Micromechanics arguments will be retained only qualitatively when dealing with damage deactivation effects (microcrack closure) and the associated friction effects.

In Table 2 are indicated the expressions chosen for the non-damage surfaces, that serve of damage loading surfaces. For the scalar variables, we consider coupled multicriteria. For the tensorial damage there is a combination of isotropic and purely anisotropic effects (by means of parameter χ) and a provision for a special shape change that will be explained below (by means of parameter ζ).

Let us remark that the present theory, thanks to the normality and to the expression for the thermodynamic force $\boldsymbol{y}$ (see Table 2), allows to develop the tensorial

Table 2
Dissipative potential, damage loading functions and normality assumption

$$f_\alpha = g_\alpha\left(\sum_\beta a_{\alpha\beta}\langle y_\beta\rangle\right) - \frac{\delta_\alpha}{D_c^\alpha} \leqslant 0 \tag{6}$$

$$f = g\big(\chi(\boldsymbol{y}^+ : \boldsymbol{Q} : \boldsymbol{y}^+)^{1/2} + (1-\chi)\operatorname{Tr}(\boldsymbol{y})\big) - \frac{\zeta \operatorname{Tr}(\boldsymbol{d}) - (1-\zeta)\operatorname{Tr}(\boldsymbol{y}.\boldsymbol{d})}{D_c} \leqslant 0 \tag{7}$$

g（y）的表达式是人为给定的，见公式（9）。

$$\dot\delta_\alpha = \dot\mu_\alpha \frac{\partial f_\alpha}{\partial y_\alpha} \qquad \dot{\boldsymbol{d}} = \dot\mu \frac{\partial f}{\partial \boldsymbol{y}} \tag{8}$$

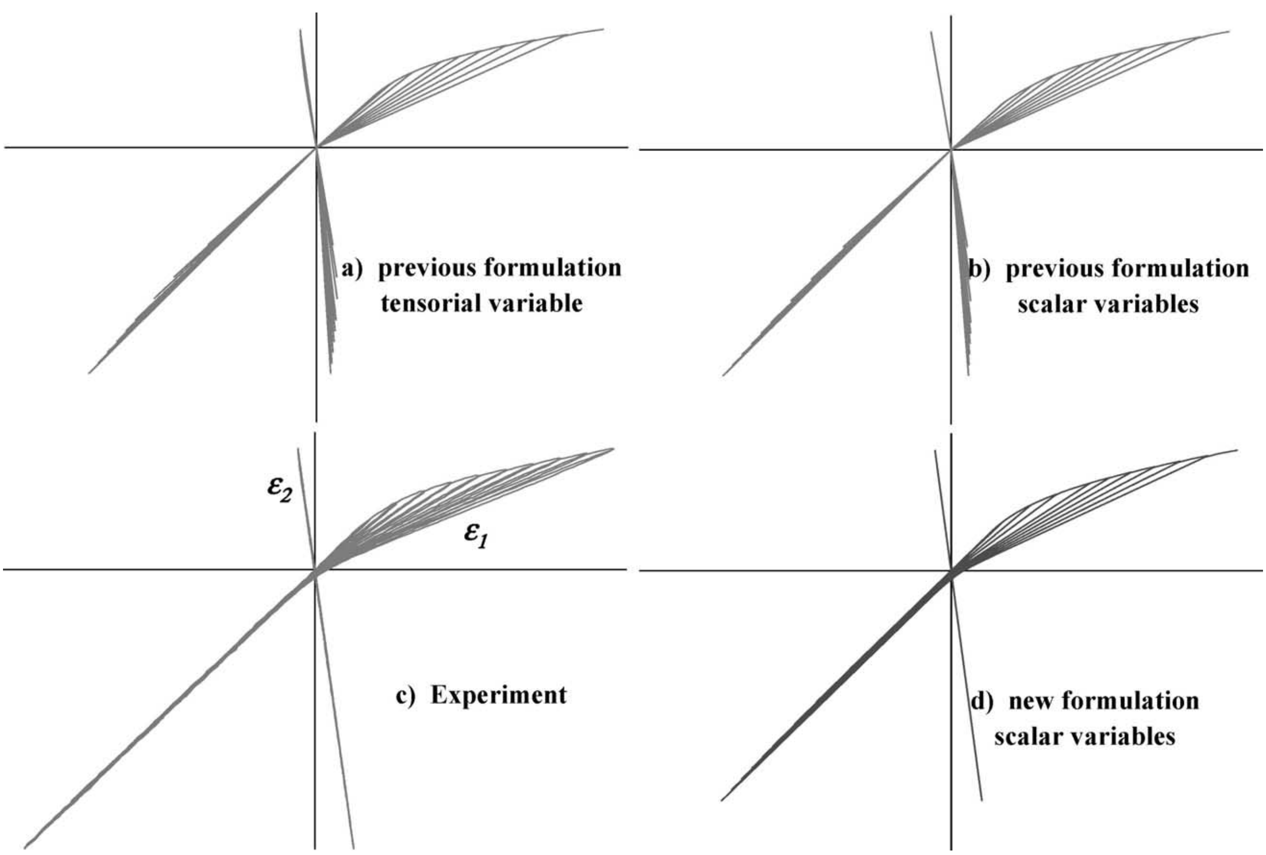

Fig. 1. Tension-compression on SiC/SiC in the direction 0–90°. (a) previous model with one tensorial variable; (b) previous model with only scalar variables; (c) experiment; (d) new formulation with only scalar variables.

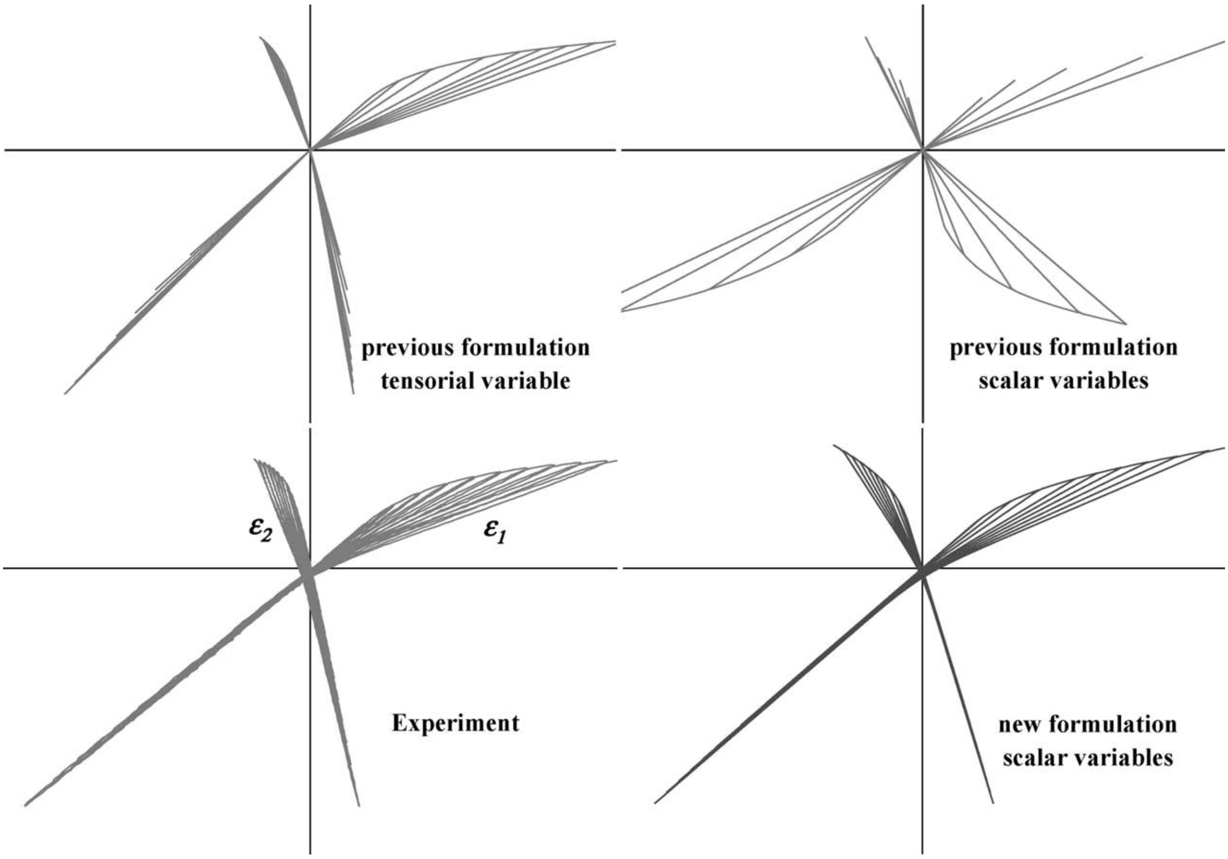

Fig. 2. Tension-compression on SiC/SiC in the direction 45°: (a) previous model with one tensorial variable; (b) previous model with only scalar variables; (c) experiment; (d) new formulation with only scalar variables.

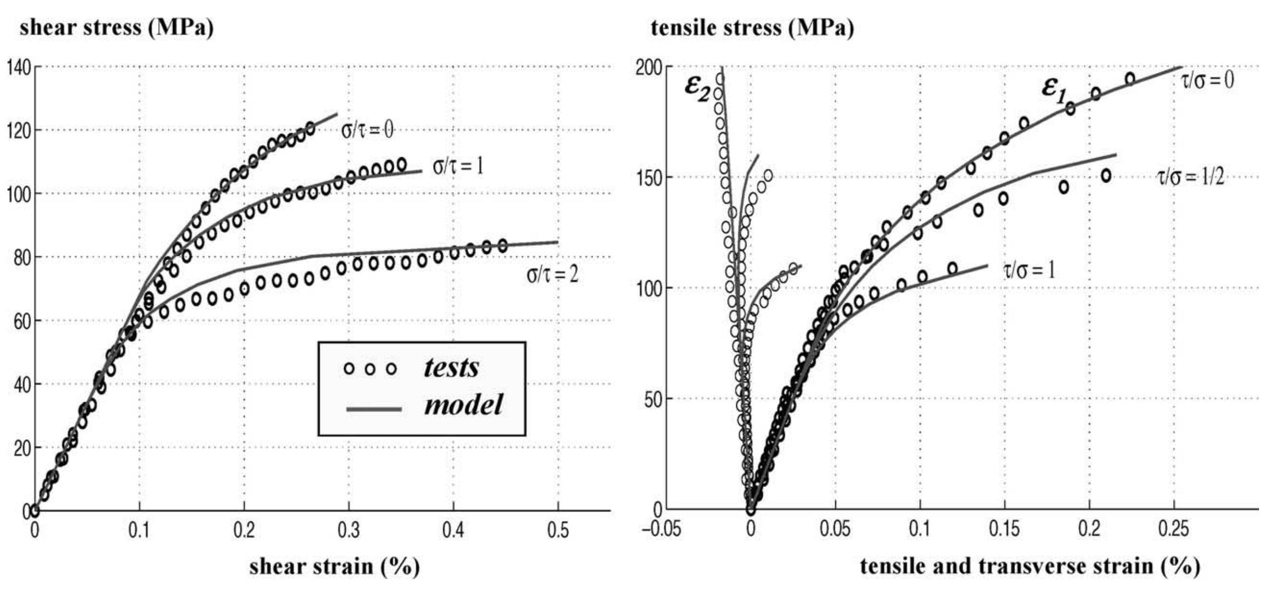

Fig. 3. Tension-torsion tests on SiC/SiC. Tensile and shear responses for 4 loading ratios.

damage $\boldsymbol{d}$ with varying principal directions (if the applied strain has varying directions). Then the damage directions are no longer with the same symmetries of the initial material, and the initial orthotropy is loosed due to this tensorial variable.

2.1. Application to a SiC/SiC material

The capabilities of the constitutive model, which general lines were presented just above, can be evaluated from a very complete experimental study made on a SiC/SiC composite
上述本构模型可以通过复杂的试验获得模型的参数。

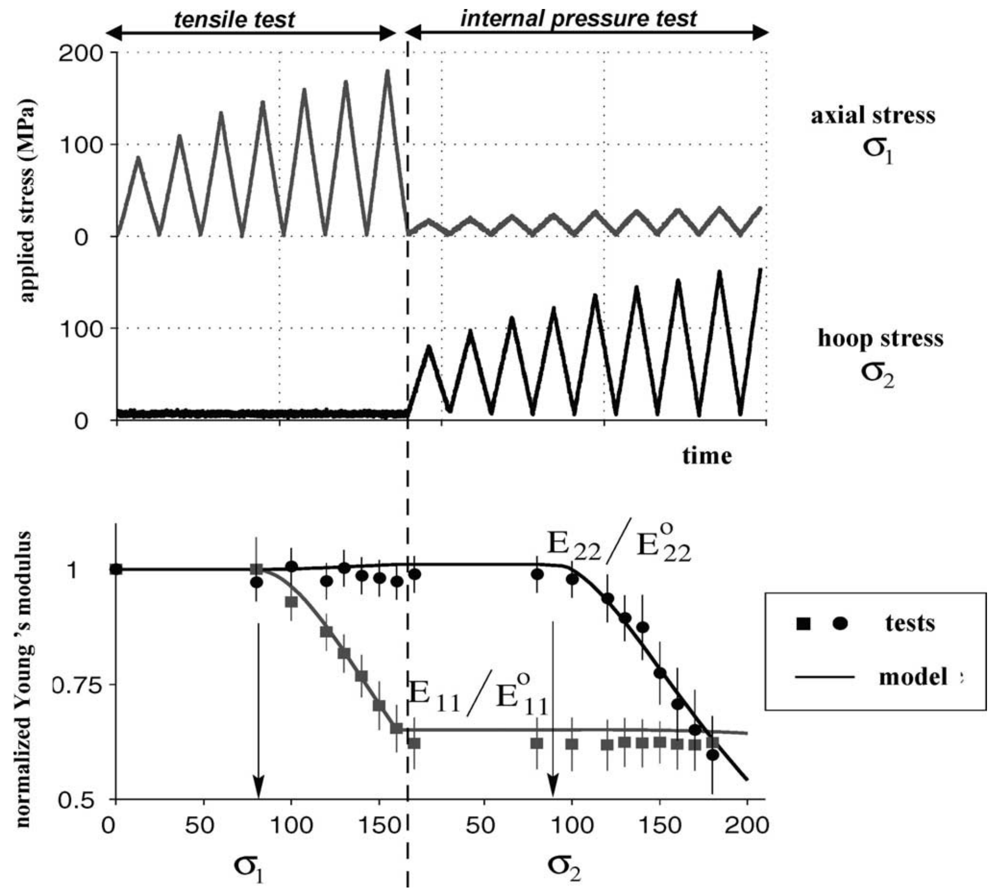

Fig. 4. Prediction of the variation of Young's modulus (directions 1 and 2) on SiC/SiC for incremental tensile loading cycles followed by incremental internal pressure loadings.

material. This one (CERASEP ® 347) was manufactured by SEP, in the context of a Brite-Euram project (BE 5462) [31], including tension-compression specimens as well as tubular specimens that allowed to perform tension/torsion and tension/internal pressure tests. The material is a woven system, composed of plain weaves with equilibrated 0 and 90° directions, so that it can be considered as initially orthotropic and symmetric. As observed in many experiments [28], the microcracks develop with the following sequence: (1) matrix cracks initiate, mainly on porosities, and grow more or less perpendicular to the maximum principal stress. These cracks also propagate in the longitudinal bundles, with fiber bridging that induces dissipation effects by friction; (2) transverse cracking in the bundles, with microcracks parallel to the fibers; (3) when these two systems of cracks are saturated, a third one develops, as longitudinal cracks, either parallel to fibers inside the longitudinal yarns or interlaminar cracks. Such observations are also confirmed by the complete measures of stiffness evolutions, as made by ultrasonic methods [2].

The model presented in Section 2 has been identified, from tensile tests at 0° and 45° only, including unloading parts and transverse strain measurements. It is one specificity of the Onera model to describe the damage induced change in the transverse compliance for the 45° direction, which allows its complete determination without using multiaxial results. The damage evolution functions in (6) and (7) have been taken of the following form, in order to incorporate saturation effects, commonly observed in composites:

$$g(y) = 1 - \exp\left(-\left\langle \frac{\sqrt{y} - \sqrt{y_o}}{\sqrt{y_c}} \right\rangle^n\right). \tag{9}$$

The elastic strain at deactivation was taken as zero valued, consistently with what is commonly observed in SiC/SiC. The same model could apply also to C/SiC with a non vanishing deactivation strain, which induces residual strains after unloading during a tensile test.

Results for tension–compression tests, with increasing the load extrema every cycle, are shown in Figs. 1 and 2. On the first one are presented the results for the direction 0–90° (tension-compression parallel to the yarns). Figs 1(c) 图1的计算结
and 1(a) respectively show the experiment and the applica- 果只采用一个
tion of the model with only one tensorial variable, including the damage deactivation responses (in compression) that will be discussed in next section. Figs. 2(c) and 2(a) show the same results for the direction 45° (tension-compression at 45° of the yarn direction). In the two cases the modeling can be improved if incorporating a combination of one tensor and three scalar variables as indicated in Section 2. 损伤张量。

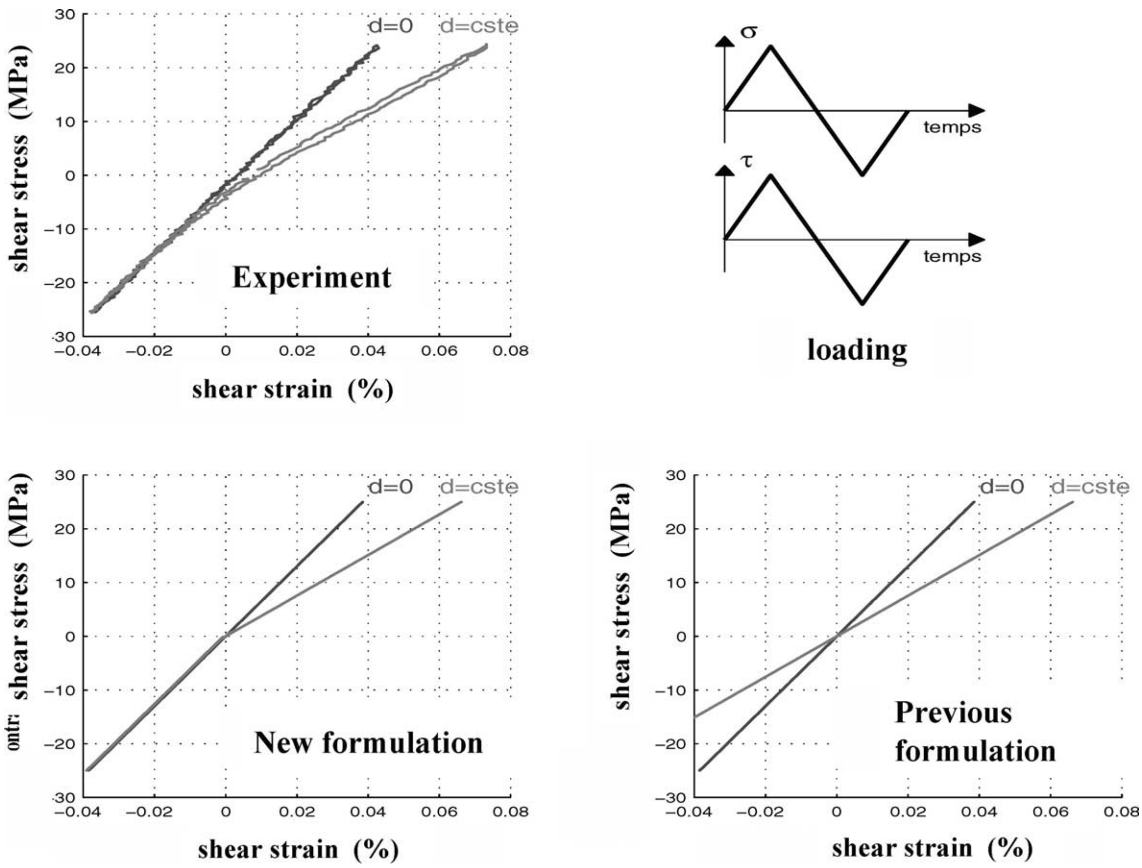

Fig. 5. Proportional tension/torsion cyclic loading, showing the shear modulus damage deactivation for compression: (a) experiment, (b) new formulation, (c) previous formulation.

图3 拉纽试验，文献[31]

Moreover, the model capabilities (for active damage conditions) have been checked under several complex multiaxial conditions, thanks to a very complete experimental study realized on tubular specimens at room temperature [31]. Fig. 3 shows the prediction of combined tension-shear experiments for four stress ratios (including pure tension and pure shear). The model predictions are extremely good in any case, both for axial, transverse and shear responses.

图4 管型试件内压，拉伸实现双轴拉伸。

The biaxial tension/internal pressure test on a tubular specimen, shown on Fig. 4, corresponds to cyclically repeated tensile loading (with increasing maxima), continued by internal pressure loading also at increasing levels (compression compensated in order to eliminate end effects). These tests were designed in order to represent biaxial tensile loading sequences with two successive uniaxial conditions in orthogonal directions.

The lower part of the figure shows an excellent agreement between the calculated and measured elasticity modulus (measured by small biaxial intermediate loadings realized between each damaging loading). It can be seen that the stress level in direction 2 (hoop stress) causing the start of the drop in modulus E_{22} is only slightly higher than the initial threshold under axial tension (leading to the drop in modulus E_{11}). This test clearly shows the requirement for a combined criterion (for the tensorial damage loading function) such as given by Eq. (7) in Table 2 with $\zeta = 0$. In the reverse case ($\zeta = 1$), as in most existing tensorial damage models, the new threshold in direction 2 would have been of the order of the maximum stress attained during loading in the first direction.

3. The damage deactivation methodology

3.1. Discussion about previous damage deactivation theories

对之前的损伤不活动理论的回顾。

Damage deactivation corresponds to the initial elastic stiffness partial or complete recovery when microcracks close under a reverse loading (compressive like loading). Those cracks that were developing and opening under the previous tensile like loading are more or less progressively closed by the subsequent unloading. We have not to confuse that problem with the one that corresponds with the non-symmetric behavior, easier to model, between tensile and compressive damaging loadings. One of the first attempts to describe damage deactivation was done by Lemaitre and Ladevèze [27], in the particular case of a scalar damage variable. A more general framework was already proposed by Ladevèze [24] in an Internal Report, which main lines were presented in a Conference [25], though the proceeding appeared only in 1993.

More difficult problems arise for non-scalar damage descriptions, associated with damage vectors [23], second order damage tensors [34], fourth order damage tensors [18,20]. Most of them were discussed by Chaboche [6–8], showing either non symmetric damaged elastic stiffness (Hooke's law not deriving from a potential) or possibilities for first order discontinuities in the stress-strain response when damage deactivation takes place under non proportional multiaxial loadings. The same problems were recognized by Carol and Willam [4] who used the terminology of a 'spurious' energy dissipation. The other framework that preserves stress-strain response continuity is Ladevèze's approach, using a spectral decomposition of the effective stress (the stress 'amplified' by the damage tensor). However this theory presents also some shortcomings, like abnormal nonlinear responses when deactivation takes place [30].

For these reasons the models developed at Onera till the recent years, mainly for composite materials, were built up on a special deactivation rule [6,8]. This one enforce the stress-strain continuity by a deactivation effect that is limited to the principal stiffness terms (the corresponding 'diagonal terms') expressed in the damage principal axes, using projection operators. Such a condition has been shown later [13] to be the only one able to respect continuity in the context of a purely bi-linear elastic behavior. Though introduced slightly different arguments, the same deactivation condition was also used by Dragon et al. [14,16,17] in the context of soil mechanics applications. The elastic potential and the corresponding state laws are indicated in Table 3 for the model that incorporates this previous deactivation rule. Projection operators are used, both for the scalar and tensorial damage models, in order to select in the deactivation rule the stiffness 'diagonal terms', which are multiplied by the corresponding strain component that vanishes when deactivation takes place.

The damage deactivation rule previously used at Onera [29] was suffering of some shortcomings, related with the limitation of deactivation effects to the principal stiffness. Some of these limitations are discussed just below, by comparison with test results obtained on the SiC/SiC composite material (Fig. 6).

– The shear modulus (in the principal damage axes) is not deactivated at all, which means a perfect sliding of the closed crack lips, a not very realistic assumption. Fig. 5 shows a combined tension/torsion cyclic loading realized on the SiC/SiC material. Experiment (Fig. 5(a)) clearly indicates that microcracks created by the first shear, combined with tensile loading, close during reverse portion, due to the compressive load, and that the initial shear stiffness is partially recovered. The previous formulation (Fig. 5(c)) was not able to model such a stiffness recovery;
– Fig. 6 illustrates the same fact differently: after initially damaging under tension, in the 0° direction of the woven fabric, we can expect microcracks perpendicular to the tensile axis. The shear response under a slightly positive tension shows a considerable reduction in shear modulus. This reduction is slightly less pronounced for negative shear, which means that additional microcracks, longitudinal or at 45°, have developed during positive shear. Contrarily, under a slight axial compression (Fig. 6(b)), for both shear direction the shear stiffness is partly recovered (here also we have the residual effect of some cracks not closed by the compressive loading).
– the tension-compression in the 45° direction (relative to the woven fabric orientation) is also an indicator of the previous model limitations (see Fig. 2): in case of a purely tensorial model principal damage directions coincide with the principal stress system: there are slight deficiencies in the model response for compressive side (Fig. 2(c)), compared with experiments (especially some abnormal stiffening, larger than the initial stiffness). Contrarily, in case of a purely scalar damage model, in which cracks are developing parallel to the yearns (at 45° of the tensile direction), we have a completely incorrect response (Fig. 2(d)), with damage even increasing under compressive loads. This is an artefact, because the normal version of the model was combining both

Table 3
State equations of the previous formulation of damage deactivation

$$\psi(\varepsilon) = \frac{1}{2}\left(\varepsilon-\varepsilon^{\mathrm{th}}-\varepsilon^{\mathrm{r}}\right):\widetilde{\boldsymbol{C}}:\left(\varepsilon-\varepsilon^{\mathrm{th}}-\varepsilon^{\mathrm{r}}\right)+\frac{1}{2}\left(\varepsilon-\varepsilon^{\mathrm{c}}\right):\left(\boldsymbol{C}^{\mathrm{eff}}-\widetilde{\boldsymbol{C}}\right):\left(\varepsilon-\varepsilon^{\mathrm{c}}\right) \tag{10}$$

$$\boldsymbol{C}^{\mathrm{eff}} = \widetilde{\boldsymbol{C}}+\eta\sum_{\alpha=1}^{N}H(-\boldsymbol{p}_\alpha.\bar{\varepsilon}.\boldsymbol{p}_\alpha)\delta_\alpha\boldsymbol{P}_\alpha:\boldsymbol{K}_\alpha:\boldsymbol{P}_\alpha-\eta\sum_{i=1}^{3}H(-\boldsymbol{n}_i.\bar{\varepsilon}.\boldsymbol{n}_i)\boldsymbol{N}_i:\left[\boldsymbol{D}(\boldsymbol{d}):\boldsymbol{K}\right]_s:\boldsymbol{N}_i \tag{11}$$

$$\boldsymbol{P}_\alpha = \boldsymbol{p}_\alpha\otimes\boldsymbol{p}_\alpha\otimes\boldsymbol{p}_\alpha\otimes\boldsymbol{p}_\alpha \qquad \boldsymbol{N}_i=\boldsymbol{n}_i\otimes\boldsymbol{n}_i\otimes\boldsymbol{n}_i\otimes\boldsymbol{n}_i \qquad \bar{\varepsilon}=\varepsilon-\varepsilon^{\mathrm{c}}$$

$$\sigma = \frac{\partial\psi}{\partial\varepsilon}=\widetilde{\boldsymbol{C}}:\left(\varepsilon-\varepsilon^{\mathrm{th}}-\varepsilon^{\mathrm{r}}\right)+\left(\boldsymbol{C}^{\mathrm{eff}}-\widetilde{\boldsymbol{C}}\right):\left(\varepsilon-\varepsilon^{\mathrm{c}}\right) \tag{12}$$

$$\sigma^{\mathrm{r}} = -\frac{\partial\psi}{\partial\varepsilon^{\mathrm{r}}}=\widetilde{\boldsymbol{C}}:\left(\varepsilon-\varepsilon^{\mathrm{th}}-\varepsilon^{\mathrm{r}}\right)=\sigma-\left(\boldsymbol{C}^{\mathrm{eff}}-\widetilde{\boldsymbol{C}}\right):\left(\varepsilon-\varepsilon^{\mathrm{c}}\right) \tag{13}$$

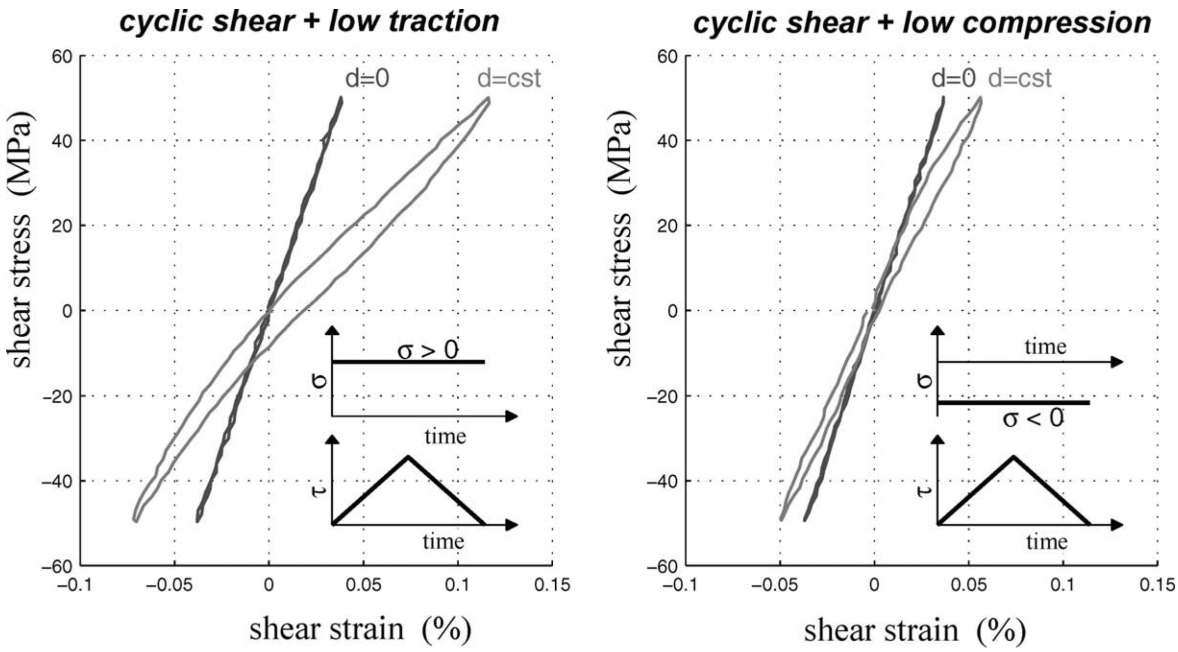

Fig. 6. Cyclic shear on SiC/SiC with a slight axial traction (left), a slight axial compression (right).

tensorial and scalar variables and was not suffering of such an extreme deficiency. However this completely abnormal behavior, indirectly produced by the limited deactivation rule, will be easily removed, even with the scalar damage version, when using the new deactivation rule proposed in Table 3.

A last difficulty was a theoretical one. When coupling the damaged elastic behavior and the deactivation effects with plasticity (as needed for example in metal matrix composites, but also in some organic matrix ones, like in C/PMR15 composites), there are two possible definitions of plastic strain and of the corresponding thermodynamic force. These two definitions were explained with more details in [10]. With the free energy chosen in Table 3, we obtain a plastic strain that is defined, at zero stress, by the elastic linear unloading, 'all damages active', eventually extrapolated to the zero stress state, as illustrated schematically on Fig. 7 for the two possible situations in tension-compression: a positive or a negative stress at deactivation. Using instead the following form for free energy:

$$\psi(\varepsilon) = \frac{1}{2}\left(\varepsilon - \varepsilon^{\mathrm{th}} - \varepsilon^{\mathrm{r}}\right) : \boldsymbol{C} : \left(\varepsilon - \varepsilon^{\mathrm{th}} - \varepsilon^{\mathrm{r}}\right) + \frac{1}{2}\left(\varepsilon - \varepsilon^{\mathrm{c}}\right) : \left(\boldsymbol{C}^{\mathrm{eff}} - \boldsymbol{C}\right) : \left(\varepsilon - \varepsilon^{\mathrm{c}}\right) \tag{14}$$

leading, by derivation, to the stress and plastic stress:

$$\sigma = \frac{\partial \psi}{\partial \varepsilon} = \boldsymbol{C} : \left(\varepsilon - \varepsilon^{\mathrm{th}} - \varepsilon^{\mathrm{r}}\right) + \left(\boldsymbol{C}^{\mathrm{eff}} - \boldsymbol{C}\right) : \left(\varepsilon - \varepsilon^{\mathrm{c}}\right), \tag{15}$$

$$\sigma^{\mathrm{r}} = -\frac{\partial \psi}{\partial \varepsilon^{\mathrm{r}}} = \boldsymbol{C} : \left(\varepsilon - \varepsilon^{\mathrm{th}} - \varepsilon^{\mathrm{r}}\right) = \sigma - \left(\boldsymbol{C}^{\mathrm{eff}} - \widetilde{\boldsymbol{C}}\right) : \left(\varepsilon - \varepsilon^{\mathrm{c}}\right) \tag{16}$$

we obtain the dual definition for plastic strain: it is defined by the linear elastic unloading, 'all damages deactivated' (from compressive side) eventually extrapolated to zero stress state, as illustrated on Fig. 8.

3.2. *Micromechanics considerations for the deactivation process*

A completely different approach will be now formulated, still in the framework of Continuum Damage Mechanics, but with some specificities directly deduced from a micromechanics analysis of microcrack closure effects [3]. We consider the schematic example of a family of parallel microcracks, in an homogeneous material volume element, submitted to a combination of tension-compression and shear loadings (Fig. 9(a)). We also assume that, under compressive closure of microcracks, friction effects are such important that sliding of crack faces is completely excluded. Then, after a tangential relative displacement of the crack faces under a slightly positive tensile stress, if we apply a slight compression we will store this tangential relative displacement, even when removing the initial shear stress.

We consider here an infinite friction coefficient, that leads to the notion of a complete deactivation. It means the complete recovery of the initial shear stiffness (as well as Poisson's transverse effects), but the corresponding stress-strain response discontinuity (if any due to the combined multiaxial loads) is 'stored' inside the material. Further stress or strain evolutions (with microcracks still closed) then store a corresponding amount of elastic energy.

In the reverse case, when microcracks re-open, following a slightly positive normal stress, this infinite friction view can induce an instantaneous stress-strain change. Fig. 9(a)

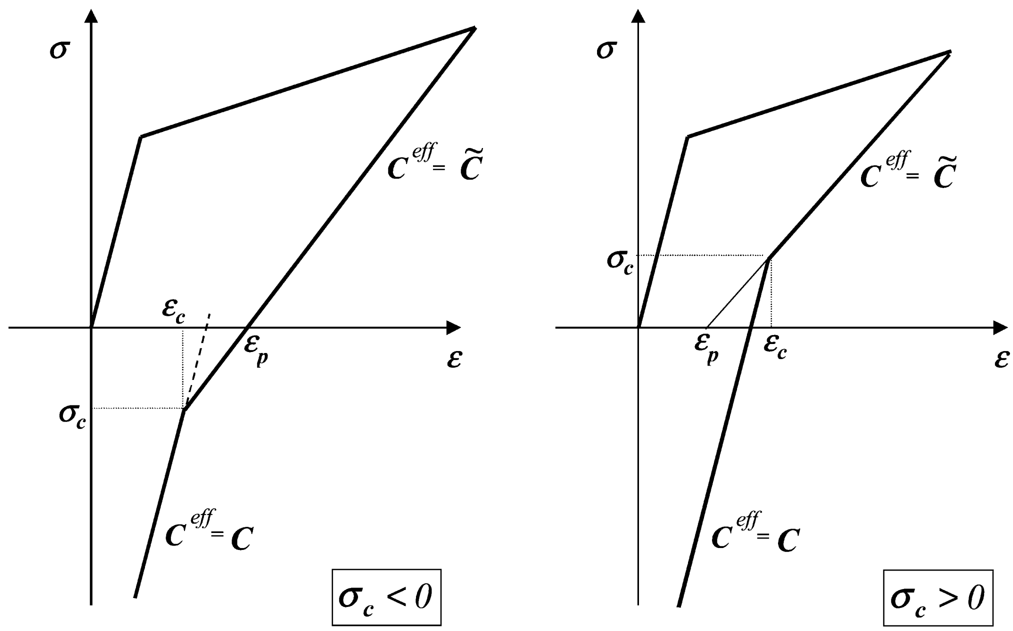

Fig. 7. Schematics of the plastic strain definition after a tensile damage ($\varepsilon^{\mathrm{th}} = 0$): (a) closure point with a negative stress; (b) closure point with a positive stress.

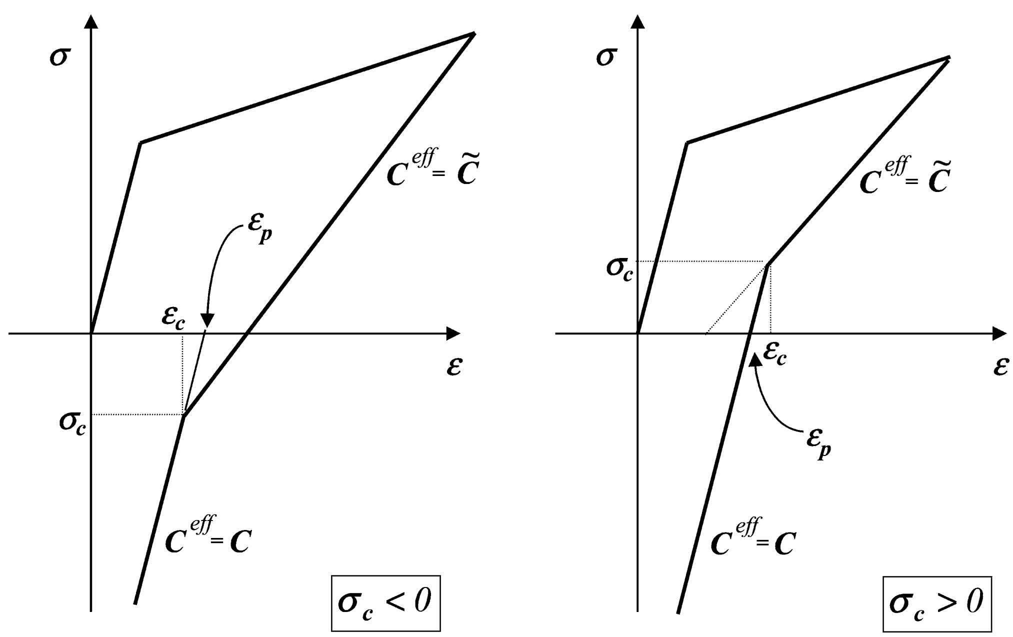

Fig. 8. Schematics of the reverse hypothesis for the plastic strain definition after a tensile damage ($\varepsilon^{\mathrm{th}} = 0$): (a) closure point with a negative stress; (b) closure point with a positive stress.

illustrates schematically the case of a positive shear under opening (small positive normal stress) followed by closure under shear (small negative normal stress). Changing the shear stress from D to E (still closed) induces an elastic energy storage. At point E, assuming a change in normal stress from negative to positive leads to a sudden shear strain release, from E to F (under a shear stress control), and the associated elastic energy release. The real case of a non infinite friction coefficient will be discussed in Section 5 (Figs. 9(b) and 9(c)).

3.3. The new deactivation formulation

The CDM new formulation of the deactivation model is given here in terms of elastic strain. For the moment we do not consider any residual or plastic strain, which can be introduced later without difficulty. The Hooke law is written with the effective stiffness $\boldsymbol{C}^{\mathrm{eff}}$ and a 'stored strain' ε^{s} that will be defined below:

$$\sigma = \boldsymbol{C}^{\mathrm{eff}} : \left(\varepsilon - \varepsilon^{\mathrm{s}}\right). \tag{17}$$

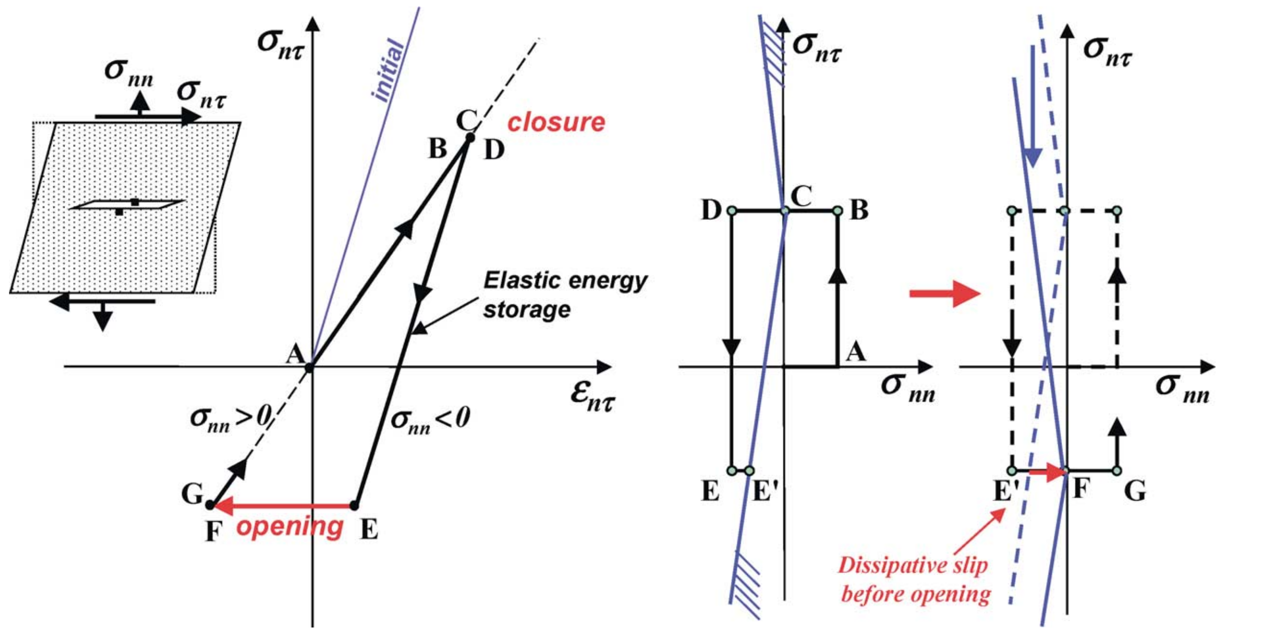

Fig. 9. Schematics of the microcrack closure effects under tension-shear combined loads: (a) shear stress-strain responses; (b) closure loading in case of a non-infinite friction; (c) opening dissipation by slip with a non-infinite friction.

We assume the deactivation criterion in terms of the elastic strain component normal to the crack. It means that $\boldsymbol{n}_\alpha$ denotes the direction normal to the crack, either the normal to the yarn (for scalar damage variables) or the principal damage direction (for tensorial damage). The deactivation criterion writes:

$$\bar{\varepsilon}_{n_\alpha} = \boldsymbol{n}_\alpha.\big(\varepsilon - \varepsilon^{\mathrm{c}}\big).\boldsymbol{n}_\alpha \leqslant 0. \tag{18}$$

If the scalar normal strain $\bar{\varepsilon}_{n_\alpha}$ is positive, the corresponding damage d_α is active; if $\bar{\varepsilon}_{n_\alpha}$ is negative, it is deactivated. The condition can be written on the effective stiffness as:

$$\boldsymbol{C}^{\mathrm{eff}} = \boldsymbol{C} - \sum_{\alpha=1}^{m} \eta_\alpha d_\alpha \boldsymbol{K}_\alpha \tag{19}$$

where $\eta_\alpha = H(\bar{\varepsilon}_{n_\alpha})$, H being the Heaviside function, and d_α meaning either a scalar damage variable or the principal value of the tensorial one, though $m = N + 3$ represents the total number of such variables. Let us explain first the case where, all damages being active, we deactivate one damage component, say d_α. Hooke's law before deactivation can be written:

$$\sigma = \boldsymbol{C}_\alpha^{(+)} : \varepsilon = \widetilde{\boldsymbol{C}} : \varepsilon \tag{20}$$

and after deactivation it is replaced by:

$$\sigma = \boldsymbol{C}_\alpha^{(-)} : \big(\varepsilon - \varepsilon_\alpha^{\mathrm{s}}\big), \tag{21}$$

where $\boldsymbol{C}_\alpha^{(-)} = \widetilde{\boldsymbol{C}} + d_\alpha \boldsymbol{K}_\alpha$. Let us assume that deactivation takes place at $\varepsilon = \varepsilon_\alpha^{\mathrm{f}}$. The stress-strain response discontinuity is prevented by combining (20) and (21) in order to determine the "stored strain" $\varepsilon_\alpha^{\mathrm{s}}$:

$$\sigma_\alpha^{\mathrm{f}} = \boldsymbol{C}_\alpha^{(+)} : \varepsilon_\alpha^{\mathrm{f}} = \boldsymbol{C}_\alpha^{(-)} : \big(\varepsilon_\alpha^{\mathrm{f}} - \varepsilon_\alpha^{\mathrm{s}}\big), \tag{22}$$

$$\varepsilon_\alpha^{\mathrm{s}} = \big[I - \big(\boldsymbol{C}_\alpha^{(-)}\big)^{-1} : \boldsymbol{C}_\alpha^{(+)}\big] : \varepsilon_\alpha^{\mathrm{f}}. \tag{23}$$

After deactivation, we have the elastic energy storage for any further strain change. Considering the free energy as $\psi_\alpha^{\mathrm{f}} = \frac{1}{2}\varepsilon_\alpha^{\mathrm{f}} : \widetilde{\boldsymbol{C}} : \varepsilon_\alpha^{\mathrm{f}}$ just at deactivation, we obtain its subsequent evolution by integrating (21) with a constant $\varepsilon_\alpha^{\mathrm{s}}$:

$$\begin{aligned}\psi(\varepsilon) &= \psi_\alpha^{\mathrm{f}} + \int_{\varepsilon_\alpha^{\mathrm{f}}}^{\varepsilon} \sigma(\varepsilon) : \mathrm{d}\varepsilon \\ &= \frac{1}{2}\big(\varepsilon - \varepsilon_\alpha^{\mathrm{s}}\big) : \boldsymbol{C}_\alpha^{(-)} : \big(\varepsilon - \varepsilon_\alpha^{\mathrm{s}}\big) + \psi_\alpha^{\mathrm{s}}.\end{aligned} \tag{24}$$

The energy stored at closure is defined by the last term, that can be rearranged successively as:

$$\begin{aligned}\psi_\alpha^{\mathrm{s}} &= \frac{1}{2}\varepsilon_\alpha^{\mathrm{f}} : \widetilde{\boldsymbol{C}} : \varepsilon_\alpha^{\mathrm{f}} - \frac{1}{2}\big(\varepsilon_\alpha^{\mathrm{f}} - \varepsilon_\alpha^{\mathrm{s}}\big) : \boldsymbol{C}_\alpha^{(-)} : \big(\varepsilon_\alpha^{\mathrm{f}} - \varepsilon_\alpha^{\mathrm{s}}\big) \\ &= \frac{1}{2}\sigma_\alpha^{\mathrm{f}} : \varepsilon_\alpha^{\mathrm{s}} \\ &= \frac{1}{2}\sigma_\alpha^{\mathrm{f}} : \big(\widetilde{\boldsymbol{C}}^{-1} - \boldsymbol{C}_\alpha^{(-)^{-1}}\big) : \sigma_\alpha^{\mathrm{f}} \\ &= \frac{1}{2}\varepsilon_\alpha^{\mathrm{s}} : \big(\widetilde{\boldsymbol{C}}^{-1} - \boldsymbol{C}_\alpha^{(-)^{-1}}\big)^{-1} : \varepsilon_\alpha^{\mathrm{s}}.\end{aligned} \tag{25}$$

It is the last expression that we will retain, considering $\varepsilon_\alpha^{\mathrm{s}}$ as the additional state variable (when damage d_α is deactivated). The free energy then writes:

$$\begin{aligned}\psi(\varepsilon) &= \frac{1}{2}\big(\varepsilon - \varepsilon_\alpha^{\mathrm{s}}\big) : \boldsymbol{C}_\alpha^{(-)} : \big(\varepsilon - \varepsilon_\alpha^{\mathrm{s}}\big) \\ &\quad + \frac{1}{2}\varepsilon_\alpha^{\mathrm{s}} : \big(\widetilde{\boldsymbol{C}}^{-1} - \boldsymbol{C}_\alpha^{(-)^{-1}}\big)^{-1} : \varepsilon_\alpha^{\mathrm{s}}.\end{aligned} \tag{26}$$

The generalization can be easily checked by considering successive deactivations and a recurrent proof. Let us assume that the first i damage variables have been deactivated. Hooke's law and the free energy write respectively:

$$\sigma = \boldsymbol{C}_i : (\varepsilon - \varepsilon^{\mathrm{s}}) \qquad \varepsilon^{\mathrm{s}} = \sum_{j=1}^{i} \varepsilon_j^{\mathrm{s}}, \tag{27}$$

$$\begin{aligned}\psi(\varepsilon) &= \psi_e + \psi_s \\ &= \frac{1}{2}(\varepsilon - \varepsilon^{\mathrm{s}}) : \boldsymbol{C}_i : (\varepsilon - \varepsilon^{\mathrm{s}}) \\ &\quad + \frac{1}{2}\sum_{j=1}^{i} \varepsilon_j^{\mathrm{s}} : \left(\boldsymbol{C}_{j-1}^{-1} - \boldsymbol{C}_j^{-1}\right)^{-1} : \varepsilon_j^{\mathrm{s}}.\end{aligned} \tag{28}$$

Be careful, in this generalization we have denoted $\boldsymbol{C}_o = \widetilde{\boldsymbol{C}}$, with a completely active damaged state, and $\boldsymbol{C}_m$ will be the initial stiffness $\boldsymbol{C}$, with all damages deactivated.

Remark 1. The last term can be written
$\frac{1}{2}\sum \sigma_j^{\mathrm{f}} : \varepsilon_j^{\mathrm{s}} = \frac{1}{2}\sum \sigma_j^{\mathrm{f}} : (c) : \sigma_j^{\mathrm{f}}$,
where σ_j^{f} is the stress state at deactivation of d_j. It can also be rewritten as
$\frac{1}{2}\sum \frac{1}{2d_j}\varepsilon_j^{\mathrm{s}} : \boldsymbol{H}_j^{-1} : \varepsilon_j^{\mathrm{s}}$
where $\boldsymbol{H}_j = \boldsymbol{C}_{j-1}^{-1} : \boldsymbol{K}_j : \boldsymbol{C}_j^{-1}$ (symmetric by construction) is the compliance difference $\Delta \boldsymbol{S} = \boldsymbol{C}_{j-1}^{-1} - \boldsymbol{C}_j^{-1}$. We recover an expression similar to the one obtained by Andrieux et al. [1], also used by Hild et al. [19] in another context. In the present theory, there are also some similarities with the one developed since a few years by Dragon et al. [14,16], in the context of soil and rock mechanics. However, the deactivation effects are not so complete and the corresponding theory is written essentially for an initially isotropic material.

Remark 2. In the present context of an infinite friction the damage reactivation (or reopening of the cracks) will lead to a discontinuous strain response (see Fig. 9(a)) if the strain at reactivation of d_α is different from the one, $\varepsilon_\alpha^{\mathrm{f}}$, that was stored at deactivation.

Remark 3. The thermodynamic forces associated with damage variables are written using the principal damage axes for the tensorial variable (which are needed to express simply the deactivated stiffnesses playing role in the stored energy term ψ_s. This can be done after transforming the fourth order tensor $[\boldsymbol{D}(\boldsymbol{d}) : \boldsymbol{K}]_s$ of Table 1 in the following decomposition

$$\left[\boldsymbol{D}(\boldsymbol{d}) : \boldsymbol{K}\right]_s = \sum_{\alpha=1}^{3} d_\alpha \boldsymbol{K}^\alpha, \tag{29}$$

where d_α, $\boldsymbol{n}^\alpha$ represent respectively the principal damage values and the principal damage directions, and where the fourth order tensor $\boldsymbol{K}^\alpha$ can be expressed as:

$$\begin{aligned}\boldsymbol{K}^\alpha &= \gamma\left[(\boldsymbol{K} : \mathbf{1}) \otimes (\boldsymbol{n}^\alpha \otimes \boldsymbol{n}^\alpha) + \left(\boldsymbol{K} : (\boldsymbol{n}^\alpha \otimes \boldsymbol{n}^\alpha)\right) \otimes \mathbf{1}\right]_s \\ &\quad + \frac{\gamma - 1}{2}\left[\boldsymbol{K} : \left(\mathbf{1} \otimes (\boldsymbol{n}^\alpha \underline{\otimes} \boldsymbol{n}^\alpha)\right)\right. \\ &\quad \left. + \boldsymbol{K} : \left(\mathbf{1} \otimes (\boldsymbol{n}^\alpha \overline{\otimes} \boldsymbol{n}^\alpha)\right)\right]_s\end{aligned} \tag{30}$$

or with the components:

$$\begin{aligned}K_{ijkl}^\alpha &= \gamma(K_{ijpp}n_k n_l + K_{ppkl}n_i n_j \\ &\quad + K_{ijpq}n_p n_q \delta_{kl} + K_{pqkl}n_p n_q \delta_{ij}) \\ &\quad + \frac{\gamma - 1}{2}(K_{ipkl}n_j n_p + K_{jpkl}n_i n_p \\ &\quad + K_{ijkp}n_p n_l + K_{ijlp}n_p n_k).\end{aligned}$$

With these notations at hand, the damage forces express easily in the same format both for scalar and tensorial variables. They write in two parts. The first one corresponds with the classical driving term (elastic energy release rate), the second one with the variation of deactivation stored energy when some (other) damage variables have been deactivated:

$$y_\alpha = y_\alpha^{\mathrm{e}} + y_\alpha^{\mathrm{s}} = \frac{1}{2}\eta_\alpha(\varepsilon - \varepsilon^{\mathrm{s}}) : \boldsymbol{K}^\alpha : (\varepsilon - \varepsilon^{\mathrm{s}}) + y_\alpha^{\mathrm{s}}, \tag{31}$$

$$\begin{aligned}y_\alpha^{\mathrm{s}} &= \frac{1}{2}\sum_{j=1}^{\alpha-1} \sigma_j^\omega : \left(\boldsymbol{C}_{j-1}^{-1} : \boldsymbol{K}^\alpha : \boldsymbol{C}_{j-1}^{-1}\right. \\ &\quad \left. - \boldsymbol{C}_j^{-1} : \boldsymbol{K}^\alpha : \boldsymbol{C}_j^{-1}\right) : \sigma_j^\omega \\ &\quad + \frac{1}{2}\sigma_\alpha^\omega : \boldsymbol{C}_{\alpha-1}^{-1} : \boldsymbol{K}^\alpha : \boldsymbol{C}_{\alpha-1}^{-1} : \sigma_\alpha^\omega,\end{aligned} \tag{32}$$

where the j indices have been ordered by the successive deactivations: d_1 first, then $d_2, \ldots, d_\alpha, \ldots, d_m$ (with $m = N + 3$). The stress σ_j^ω represents the corresponding stress at deactivation:

$$\sigma_j^\omega = \left(\boldsymbol{C}_{j-1}^{-1} - \boldsymbol{C}_j^{-1}\right)^{-1} : \varepsilon_j^{\mathrm{s}}. \tag{33}$$

Let us note here the approximation about neglecting the change of the tensorial damage principal directions when writing the part of elastic stored energy release. In fact it is easy to check that the y_α^{s} is significantly lower than y_α^{e} in situations where damage is increasing (but with some damage component deactivated). Then, it is anticipated that neglecting this variation on a low part of y_α will not affect the positiveness of dissipation.

Remark 4. The thermal expansion $\varepsilon^{\mathrm{th}}$, and the residual strain ε^{r} (or plastic strain) can now be implemented. This is done in Table 4, in the framework of general notations, not repeating the expression for ψ_s, given in (28):

$$\psi_s = \frac{1}{2}\sum_{j=1}^{i} \varepsilon_j^{\mathrm{s}} : \left(\boldsymbol{C}_{j-1}^{-1} - \boldsymbol{C}_j^{-1}\right)^{-1} : \varepsilon_j^{\mathrm{s}}. \tag{34}$$

The thermodynamic conjugate forces follow easily as in Remark 3. We can define the conjugate of the strain $\varepsilon_j^{\mathrm{s}}$ stored by deactivation as:

$$\sigma_{mj}^{\mathrm{s}} = \frac{\partial \psi}{\partial \varepsilon_j^{\mathrm{s}}} = \left(\boldsymbol{C}_{j-1}^{-1} - \boldsymbol{C}_j^{-1}\right)^{-1} : \varepsilon_j^{\mathrm{s}} - \sigma = \sigma_j^\omega - \sigma. \tag{35}$$

Table 4
State equations of the new formulation with the instantaneous deactivation rule

$\psi(\varepsilon) = \frac{1}{2}\left(\varepsilon-\varepsilon^{\mathrm{th}}-\varepsilon^{\mathrm{r}}-\varepsilon^{\mathrm{s}}\right):\boldsymbol{C}^{\mathrm{eff}}:\left(\varepsilon-\varepsilon^{\mathrm{th}}-\varepsilon^{\mathrm{r}}-\varepsilon^{\mathrm{s}}\right)+\psi_s\left(\boldsymbol{d}^{\mathrm{eff}},\eta_\alpha\delta_\alpha,\varepsilon^{\mathrm{s}}\right)$	(36)
$\boldsymbol{C}^{\mathrm{eff}} = \boldsymbol{C}-\sum_{\alpha=1}^{m}\eta_\alpha\delta_\alpha\boldsymbol{K}_\alpha-\left[\boldsymbol{D}\left(\boldsymbol{d}^{\mathrm{eff}}\right):\boldsymbol{K}\right]_s \qquad \boldsymbol{d}^{\mathrm{eff}}=\sum_{i=1}^{3}\eta_i d_i\boldsymbol{n}_i\otimes\boldsymbol{n}_i$	(37)
$\eta_i = H\left(\boldsymbol{n}_i.(\varepsilon^{\mathrm{e}}-\varepsilon^{\mathrm{c}}).\boldsymbol{n}_i\right) \qquad \eta_\alpha=H\left(\boldsymbol{p}_\alpha.(\varepsilon^{\mathrm{e}}-\varepsilon^{\mathrm{c}}).\boldsymbol{p}_\alpha\right) \qquad \varepsilon^{\mathrm{e}}=\varepsilon-\varepsilon^{\mathrm{th}}-\varepsilon^{\mathrm{r}}$	(38)

4. Applications on the SiC/SiC composite

4.1. Application to special test conditions

The proposed new deactivation rule has been incorporated into the SiC/SiC model. The thermodynamic forces associated with damage are modified according to (28) and contain additional terms related to the stored energy. However there is practically no change for the normal (active) loading conditions, so that the damage loading surfaces and the material parameters are unmodified. The main differences can be observed under the special test conditions that were already discussed in Section 4.1.

Let us begin by the extreme situation where we do implement only the scalar damage variables. In that case, the completely inoperative results of the previous formulation are clearly eliminated (see Fig. 2) and a quite good modeling of the 45° tension-compression experiments is now easily possible (Fig. 2(d)). In the 0° direction the modeling is also excellent (Fig. 1(d)), with no effect of damage deactivation on the transverse strain (contrary to the previous formulation).

In the cyclic tests in combined tension/torsion (proportional) for example, the new formulation also leads to a much more acceptable result (Fig. 5(b)) compared to the previous formulation. Other test conditions under complex tension/torsion have also shown good predictions with this deactivation new rule.

4.2. A formulation with a progressive deactivation

In actual situations the deactivation effects are not playing role instantaneously as bilinear elastic responses. In fact, actual microcracks, with some randomness in their orientations, close progressively, which renders much more continuous the macroscopic behavior. A progressive deactivation rule has been formulated that replaces the Heaviside functions of the deactivation criterion (18) by a progressive evolution of the deactivation index η [33].

The formulation is built up into the thermodynamic framework, considering as a particular case the above formulation with an instantaneous deactivation. We limit ourselves to the case of scalar variables. Except notation difficulties, the theory can easily be generalized with a damage tensor [33]. We assume several internal state variables:

- the damage variables themselves, $\delta_\alpha,\ \alpha=1,2,\ldots,N$;
- the deactivation indexes $\eta_\alpha,\ \alpha=1,2,\ldots,N$, associated with each scalar damage variable. They take the values 1 when damage is active, and 0 when damage is completely deactivated;
- the associated stored strains $\varepsilon_j^{\mathrm{s}}$, that are stored progressively when deactivation progresses.

Equations of state of this model are the same than for the instantaneous deactivation. We have assumed exactly the same form as previously for the free energy, including the stored strains $\varepsilon_j^{\mathrm{s}}$ and $\varepsilon^{\mathrm{s}}=\sum\varepsilon_j^{\mathrm{s}}$. In the additional stored energy terms in the free energy we use the successive stiffnesses $\boldsymbol{C}_j$ for completely deactivated damage δ_j, assuming in the notations that the deactivation is ordered, which means:

$$0\leqslant\eta_1\leqslant\eta_2\leqslant\cdots\leqslant\eta_N\leqslant 1.$$

Provided index factors and damage variables are considered as independent state variables, the corresponding two sets of thermodynamic forces, y_α and χ_α, express independently. (31) stands for y_α and we have similar relations for χ_α:

$$\chi_\alpha=\frac{1}{2}\delta_\alpha\left(\varepsilon-\varepsilon^{\mathrm{s}}\right):\boldsymbol{K}^\alpha:\left(\varepsilon-\varepsilon^{\mathrm{s}}\right). \tag{39}$$

For the forces associated with the (now continuous) stored elastic strains $\varepsilon_j^{\mathrm{s}}$, we can easily demonstrate that they still correspond with:

$$\sigma_j^{\mathrm{s}}=\sigma_j^{\omega}-\sigma \tag{40}$$

where $\sigma_j^{\omega}=(\boldsymbol{C}_{j-1}^{-1}-\boldsymbol{C}_j^{-1})^{-1}:\varepsilon_j^{\mathrm{s}}$ is now the stress at deactivation in the corresponding instantaneous deactivation (Fig. 10(b)). The damage evolution equations are unmodified. The other evolution equations concern:

– 'The evolution of the deactivation index', from 1 to 0, during the deactivation process (from 0 to 1 in the reverse situation). We still use the criterion in terms of the normal elastic strain $\bar{\varepsilon}_{n_j}=\boldsymbol{n}_j.(\varepsilon-\varepsilon^{\mathrm{c}}).\boldsymbol{n}_j$. Instead of the discontinuous jump with the Heaviside function, we assume an evolution like

$$\dot{\eta}_j=\hat{\eta}(\bar{\varepsilon}_{n_j})\dot{\bar{\varepsilon}}_{n_j}, \tag{41}$$

where the function $\hat{\eta}$ is chosen with the following properties: $\hat{\eta}\geqslant 0$; $\hat{\eta}$ vanishes for large values of $|\bar{\varepsilon}_{n_j}|$; $\hat{\eta}(x)$ is maximum at $x=0$. For instance we can choose $\hat{\eta}(x)=\frac{1}{2}c\exp(-c|x|)$, so that, after integrating (41) above, we find

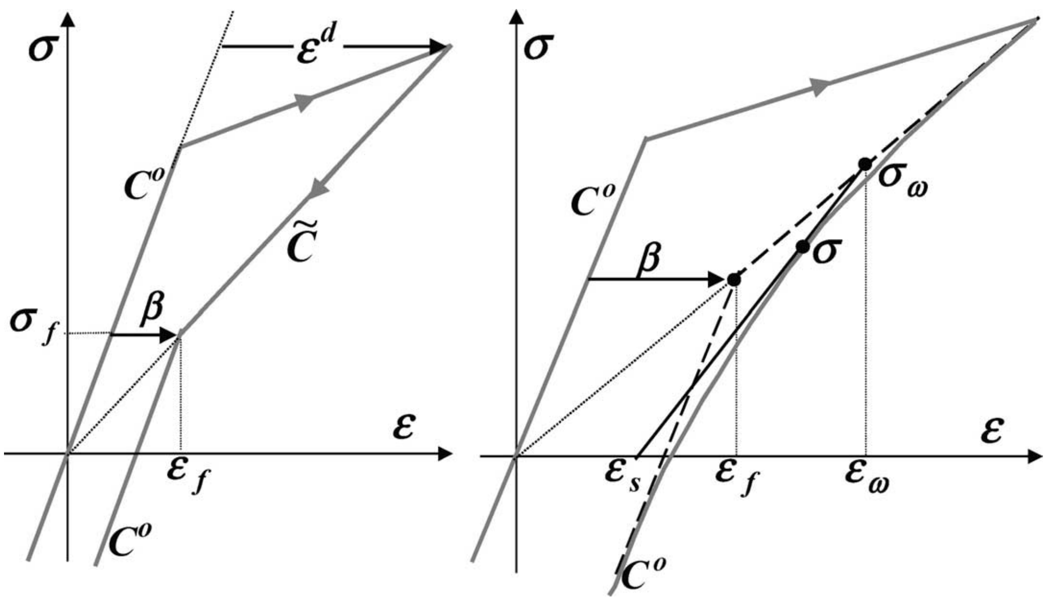

Fig. 10. Schematics of the new deactivation rule: (a) instantaneous deactivation; (b) progressive deactivation.

$\eta(x) = \frac{1}{2} + \frac{1}{2}(1 - \exp(-c|x|))\mathrm{sgn}(x)$, a function with the correct properties (1 for large positive values of x; 0 for large negative values, $1/2$ at $x = 0$). Parameter c can be made dependent on the accumulated damage δ_j.

– 'The evolution of the stored strains': they must evolve continuously from 0 to the strain that corresponds with the complete deactivation (strain β_j of the model with instantaneous deactivation). Fig. 10(b) illustrates schematically how $\varepsilon_j^{\mathrm{s}}$ increases as the effective stiffness (tangent) increases. Let us remark some similarities in the present model with a work done by Gerard and Baste [15]. Because it is normal to consider that damage deactivation is a non-dissipative process (at least when friction effects are not taken into account), we decide here to enforce dissipation to be zero independently for each deactivation mechanism, which means:

$$-\frac{\partial\psi}{\partial\varepsilon_j^{\mathrm{s}}} : \dot{\varepsilon}_j^{\mathrm{s}} - \frac{\partial\psi}{\partial\eta_j} : \dot{\eta}_j = -\sigma_j^{\mathrm{s}} : \dot{\varepsilon}_j^{\mathrm{s}} - \chi_j : \dot{\eta}_j = 0. \tag{42}$$

To choose $\dot{\varepsilon}_j^{\mathrm{s}}$ to be collinear with σ_j^{s} is a logical assumption, so that this condition writes:

$$\dot{\varepsilon}_j^{\mathrm{s}} = -\frac{\chi_j : \dot{\eta}_j}{\sigma_j^{\mathrm{s}} : \sigma_j^{\mathrm{s}}}\sigma_j^{\mathrm{s}}. \tag{43}$$

This assumption of zero dissipation is well justified for the deactivation situation. In case of reactivation, we consider a reversible behavior, so that the same model apply: the index η_j evolves from 0 to 1 (still driven by the normal strain that changes from a negative to a positive value), and the stored strain $\varepsilon_j^{\mathrm{s}}$ progressively vanishes.

In fact, as shown below, such a behavior could lead to incorrect results for complex multiaxial loadings (non-proportional). We will see that, in case of damage reactivation (reopening of cracks) we should expect a discontinuous response (instead of a continuous one) when the stress (strain) states are significantly different from those present at the deactivation stage. The continuous response when reactivation takes place is recovered only if one introduces friction effects, which means an additional dissipation, so that the dissipation should not be enforced to be zero as it was assumed in the present context.

This progressive deactivation rule has been applied for SiC/SiC tension-compression tests at 0° and 45°, as shown in Fig. 11. Only one additional material parameter was used, that governs the evolution of the deactivation indexes. It is shown that this progressive deactivation improves significantly the modeling for stresses around 0.

5. Discussion and future developments

In the present damage model of CMC's, we have incorporated most of the significant facts that must be taken into account:

– the possibility for damage development in compression for large stress levels, by splitting effects and the development of longitudinal cracks;
– the correct modeling of transverse strains in uniaxial tension-compression for directions 0° as well as 45°;
– the correct prediction of combined tension-shear experiments with various load ratio and the capability to model the significant shape change of the non-damage surface, even for the tensorial damage, as demonstrated by biaxial tests (tension-compression + internal pressure);
– the new damage deactivation rule allows now to describe correctly the complete deactivation (especially for the shear modulus), without a stress-strain response discontinuity;
– in the reverse situation of the damage re-activation it is possible to have a stress-strain response discontinuity

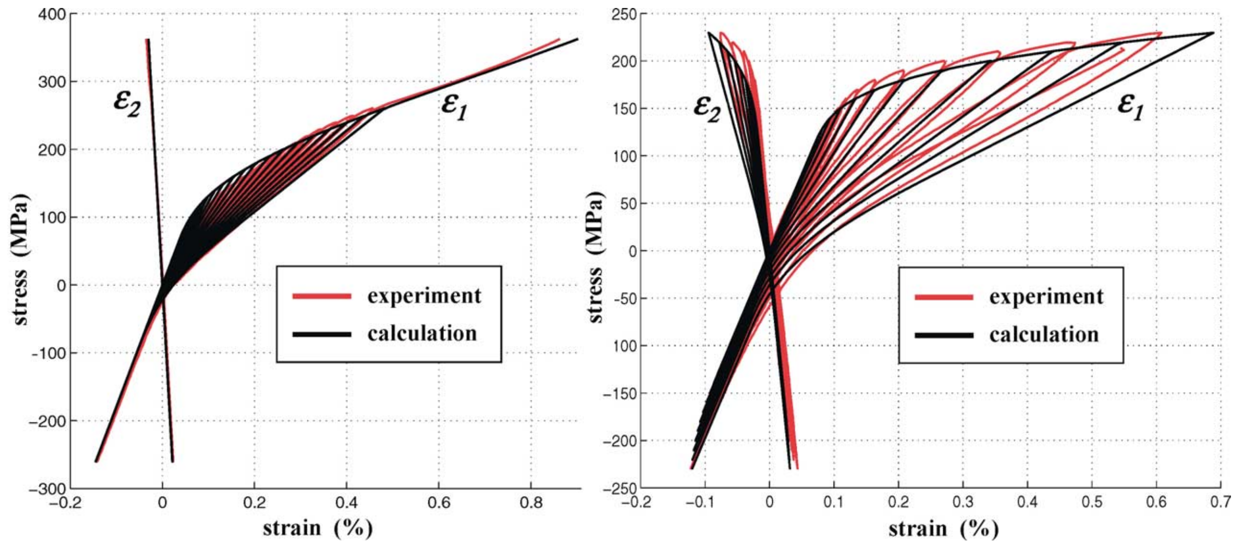

Fig. 11. Tension-compression simulation with the progressive deactivation model: (a) direction 0–90°; (b) direction 45°.

(for complex loadings in which the stress at opening is different than that at crack closing). This is expected to be in conformity with microcrack mechanics, provided friction dissipation has not been introduced;
– a progressive deactivation model has been proposed, which produces correct responses. It uses two additional internal variables submitted to the constraint of a zero dissipation during deactivation.

Clearly, the open problem that needs further modeling efforts, is related with friction effects. In that aspect, two objectives can be selected for CDM based models in composite materials:

(1) better describe the damage reactivation effects, replacing the possibility of a discontinuous stress-strain response by a sliding and dissipative effect,
(2) introduce slight inelastic hysteresis that can be observed during the quasi-elastic unloading/reloading, and therefore be able to describe the damage growth during fatigue tests.

In relation with the first objective, it is interesting to consider the microcrack example already discussed (Fig. 9(a)). Assume a shear loading with a small positive normal stress that opens the crack (AB), then change the normal stress to a negative value (BD). If the friction coefficient of crack surface faces is sufficient, the shear stress can be changed (DE), leading to a shear response that obeys the initial shear stiffness. During (DE) there is an elastic energy storage (model of Section 3.3).

Suppose now the normal stress changing to a positive value (EG). An infinite friction view will interpret the path (EF) as a discontinuous response. Contrarily, for a limited Coulomb's friction resistance, we have the behavior shown on Fig. 9(b) [1,11]: at point C, just at closure, the Coulomb cone is created. During (DE) there is no relative displacement of the crack faces. Before reopening (EG) Coulomb's criterion is necessarily attained and slip takes place from point E′ to point F, which demonstrates that the expected discontinuous response corresponds in fact to a slip mechanism and to an additional dissipation by friction.

The second objective will need to introduce additional damage and friction effects at a lower level, taking into account the bridging effects (of the matrix microcracks that have grown more or less perpendicular to the bundles) and the associated secondary debonding and friction effects. In this objective, the CDM based model will be supported by works done by Hild et al. [19].

References

[1] S. Andrieux, J.J. Marigo, Y. Bamberger, Un modèle de matériau microfissuré pour les bétons et les roches, J. de Mécanique Théorique et Appliquée 5 (3) (1986) 471–513.
[2] S. Baste, Inelastic behavior of ceramic matrix composites, Workshop on "Recent Advances in Continuum Damage Mechanics for Composites", Cachan (France), 2000.
[3] A. Boursin, J.L. Chaboche, F. Roudolff, Mécanique de l'endommagement avec conditions unilatérales et stockage d'énergie élastique, C. R. Acad. Sci. Paris, Série IIb 323 (1996) 369–376.
[4] I. Carol, K. Willam, Spurious energy dissipation/generation in stiffness recovery models for elastic degradation and damage, Int. J. Solids Structures 33 (1996) 2939–2957.
[5] J.L. Chaboche, Le concept de contrainte effective appliqué à l'élasticité et à la viscoplasticité en présence d'un endommagement anisotrope, Col. Euromech 115, Grenoble, CNRS, 1979.
[6] J.L. Chaboche, Damage induced anisotropy: on the difficulties associated with the active/passive unilateral condition, Int. J. Damage Mechanics 1 (1992) 148–171.
[7] J.L. Chaboche, Une nouvelle condition unilatérale pour décrire le comportement des matériaux avec dommage anisotrope, C. R. Acad. Sci. Paris, Série II 314 (1992) 1395–1401.
[8] J.L. Chaboche, Development of CDM for elastic solids sustaining anisotropic and unilateral damage, Internat. J. Damage Mechanics 2 (1993) 311–329.

[9] J.L. Chaboche, P.M. Lesne, J.F. Maire, Continuum Damage Mechanics, anisotropy and damage deactivation for brittle materials like concrete and ceramic composites, Internat. J. Damage Mechanics 4 (1995) 5–22.
[10] J.L. Chaboche, O. Lesné, T. Pottier, Continuum Damlage Mechanics of composites: towards a unified approach, in: G. Voyiadjis, J. Ju, J.L. Chaboche (Eds.), Damage Mechanics in Engineering Materials, Elsevier Science, Amsterdam, 1998, pp. 3–26.
[11] J.L. Chaboche, P. Suquet, Endommagement, interfaces, Ecole d'Ete "Méthodes d'Homogénéisation en Mécanique des Matériaux", La Londe-les-Maures, 1998.
[12] J.P. Cordebois, F. Sidoroff, Anisotropie élastique induite par endommagement, Col. Euromech. 115, Grenoble, CNRS, 1979.
[13] A. Curnier, Q. He, P. Zysset, Conewise linear elastic materials, J. Elasticity 37 (1995) 1–38.
[14] A. Dragon, D. Halm, Doubly dissipative model fpr quasi-brittle solids: anisotropic damage and frictional sliding on microcracks, in: A. Benallal (Ed.), Continuous Damage and Fracture, Elsevier, Amsterdam, 2000, pp. 207–215.
[15] A. Gérard, S. Baste, Comportement non linéaire des composites à matrice céramique en cycle de charge-décharge, C. R. Acad. Sci. Paris, Série II 313 (1991) 1361–1366.
[16] D. Halm, A. Dragon, A model of anisotropic damage by mesocrack growth – unilateral effects, Internat. J. Damage Mechanics 5 (4) (1996) 384–402.
[17] D. Halm, A. Dragon, An anisotropic model of damage and frictional sliding for brittle materials, Eur. J. Mech., A/Solids 17 (1998) 439–460.
[18] N.R. Hansen, H.L. Schreyer, A thermodynamically consistent framework for theories of elastoplasticity coupled with damage, Internat. J. Solids Structures 31 (3) (1994) 359–389.
[19] F. Hild, A. Burr, F.A. Leckie, Fiber breakage and fiber pull-out of fiber-reinforced ceramic-matrix composites, Eur. J. Mech., A/Solids 13 (6) (1994) 749–803.
[20] J.W. Ju, On energy-based coupled elastoplastic damage theories: constitutive modeling and computational aspects, Internat. J. Solids Structures 25 (7) (1989) 803–833.
[21] L.M. Kachanov, Time of the rupture process under creep conditions, Isv. Akad. Nauk SSR. Otd. Tekh. Nauk 8 (1958) 26–31.
[22] M. Kachanov, Elastic solids with many cracks and related problems, Adv. Appl. Mech. 30 (1993) 259–445.
[23] D. Krajcinovic, G.U. Fonseka, The continuous damage theory of brittle materials, Parts I and II, J. Appl. Mech. 48 (1981) 809–824.
[24] P. Ladevèze, Sur une théorie de l'endommagement anisotrope, Rapport Interne 34, LMT-Cachan, 1983.
[25] P. Ladevèze, On an anisotropic damage theory, in: Boehler (Ed.), Failure Criteria of Structural Media, CNRS Int. Colloquium n°351, Villard-De-Lans, Balkema, Rotterdam, 1983.
[26] P. Ladevèze, A. Gasser, O. Allix, Damage mechanics modelling for ceramic composites, J. Engrg. Mater. Technol. 116 (1994).
[27] P. Ladevèze, J. Lemaitre, Damage effective stress in quasi-unilateral material conditions, IUTAM Congress, Lyngby (Denmark), 1984.
[28] J. Lamon, Micromechanics-based approach to the mechanical behavior of brittle matrix composites, Workshop on "Recent Advances in Continuum Damage Mechanics for Composites", Cachan (France), 2000.
[29] J.F. Maire, J.L. Chaboche, A new formulation of continuum damage mechanics for composite materials, Aerosp. Sci. Technol. 4 (1997) 247–257.
[30] J.F. Maire, P.M. Lesne, A damage model for ceramic matrix composites, Aerosp. Sci. Technol. 4 (1997) 259–266.
[31] J.F. Maire, D. Pacou, Essais de traction-compression-torsion sur tubes composites céramique-céramique, in: 10èmes Journées Nationales Composites, Paris, AMAC, 1996, pp. 1361–1371.
[32] S. Murakami, Notion of continuum damage mechanics and its application to anisotropic creep damage theory, J. Engrg. Mater. Technol. 105 (1983) 99.
[33] T. Pottier, Modélisation multiéchelle du comportement et de l'endommagement de composites à matrice métallique, Thèse ENPC, 1998.
[34] S. Ramtani, Contribution à la modélisation du comportement multiaxial du béton endommagé avec description du caractère unilatéral, Thèse de Doctorat, Univ. Paris VI, 1990.
[35] R. Talreja, Continuum modelling of damage in ceramic matrix composites, Mech. Mater. 12 (1991) 165–180.
[36] A.A. Vakulenko, M.L. Kachanov, Continuum theory of medium with cracks, Mech. Solids 6 (4) (1971) 145–151, Engl. Transl. of 'Mekhanika Tverdogo Tela' (in Russian).